A Major Collapse of Kangerlussuaq Glacier's Ice Tongue Between 1932 and 1933 in East Greenland

Vermassen, Flor; Bjørk, Anders A.; Sicre, Marie Alexandrine; Jaeger, John M.; Wangner, David J.; Kjeldsen, Kristian K.; Siggaard-Andersen, Marie Louise; Klein, Vincent; Mouginot, Jeremie; Kjær, Kurt H.; Andresen, Camilla S.

Published in:
Geophysical Research Letters

DOI:
10.1029/2019GL085954

Publication date:
2020

Document version
Publisher's PDF, also known as Version of record

Geophysical Research Letters

RESEARCH LETTER
10.1029/2019GL085954

Key Points:
- Historical evidence reveals a major collapse of Kangerlussuaq Glacier's ice tongue between 1932 and 1933
- The collapse was likely triggered by increasing air and ocean temperatures during the late 1920s/early 1930s
- Compared to other glaciers in Greenland this retreat event occurred relatively late, probably due to its pinning to a large submarine moraine

Supporting Information:
- Supporting Information S1

Correspondence to:
F. Vermassen,
flor.vermassen@gmail.com

Citation:
Vermassen, F., Bjørk, A. A., Sicre, M.-A., Jaeger, J. M., Wangner, D. J., Kjeldsen, K. K., et al. (2020). A major collapse of Kangerlussuaq Glacier's ice tongue between 1932 and 1933 in East Greenland. *Geophysical Research Letters*, *47*, e2019GL085954. https://doi.org/10.1029/2019GL085954

Received 8 NOV 2019
Accepted 29 JAN 2020
Accepted article online 30 JAN 2020

A Major Collapse of Kangerlussuaq Glacier's Ice Tongue Between 1932 and 1933 in East Greenland

Flor Vermassen[1,2], Anders A. Bjørk[2], Marie-Alexandrine Sicre[3], John M. Jaeger[4], David J. Wangner[1,2], Kristian K. Kjeldsen[1], Marie-Louise Siggaard-Andersen[2], Vincent Klein[3], Jeremie Mouginot[5,6], Kurt H. Kjær[2], and Camilla S. Andresen[1]

[1]Department of Glaciology and Climate, GEUS, Copenhagen, Denmark, [2]Centre for GeoGenetics, University of Copenhagen, Copenhagen, Denmark, [3]LOCEAN, CNRS, Sorbonne Université, Campus Pierre et Marie Curie, Paris, France, [4]Department of Geological Sciences, University of Florida, Gainesville, FL, USA, [5]University Grenoble Alpes, CNRS, Grenoble, France, [6]Department of Earth System Science, University of California, Irvine, CA, USA

Abstract In recent years, several large outlet glaciers in Greenland lost their floating ice tongue, yet little is known regarding their stability over a longer timescale. Here we compile historical documents to demonstrate a major ice tongue collapse of Kangerlussuaq Glacier between 1932 and 1933. This event resulted in a 9-km retreat, exceeding any of the glacier's recent major retreat events. Sediment cores from the fjord are used to reconstruct sea surface temperatures and to investigate a potential sedimentological trace of the collapse. During the 1920s, local and regional sea surface temperatures and air temperatures increased rapidly, suggesting a climatic trigger for the collapse. Fjord bathymetry played an important role too, as the (partially) pinned ice tongue retreated off a submarine moraine during the event. This historical analogue of a glacier tongue collapse emphasizes the fragility of remaining ice tongues in North Greenland within a warming climate.

Plain Language Summary In the past two decades, multiple Greenlandic glaciers retreated because their floating part (="ice tongue") melted and broke off. While it is believed that such events are the result of a warming climate, not much is known about how often or when such events have occurred in the past. In this study, we compiled multiple historical sources to show that Kangerlussuaq Glacier, one of Greenland's largest glaciers, retreated drastically between 1932 and 1933. During this event the ice tongue collapsed, leading to a 9-km retreat, which is more than during any of the glacier's recent retreat events. By studying fjord sediments we show that the ocean temperatures increased prior to the event, as did air temperatures. Thus, climatic warming likely triggered the collapse. While other glaciers had already started their retreat decades earlier, Kangerlussuaq Glacier had been stable until 1932, probably due to stabilizing effect of an underwater moraine. Overall, this study emphasizes that ice tongues are sensitive to climatic warming and highlights the precarious position of current ice tongues in Northern Greenland.

1. Introduction

1.1. Background and Rationale

In the past two decades, mass loss from the Greenland ice sheet has increased its contribution to sea level rise, leading to a peak mass loss in 2012 equivalent to 1.2-mm sea level rise (Mouginot et al., 2019; Rignot et al., 2008; van den Broeke et al., 2016). Since the late 1990s, several large tidewater glaciers displayed sudden signs of rapid change, marked by fast retreat, thinning, and ice flow acceleration (Howat et al., 2007; Kjær et al., 2012). For example, Jakobshavn Isbræ in West Greenland retreated promptly in 1997, thereby doubling its ice velocity (Holland et al., 2008). In turn, the Helheim and Kangerlussuaq glaciers in Southeast Greenland displayed rapid retreat events in 2000–2005 and 2004–2005, respectively (Howat et al., 2005; Khan et al., 2014; Luckman et al., 2006; Rignot et al., 2004). These observations revealed that the dynamics of tidewater glaciers can change markedly over short time scales (Howat et al., 2007; Nick et al., 2009). Since these events were preceded by increased inflow of deep, warm ocean waters to the Southeast and West Greenland shelf, ocean warming has been proposed as a trigger (Christoffersen et al., 2011; Holland et al., 2008; Rignot et al., 2012; Straneo & Heimbach, 2013). In addition, variations in bed geometry have also been suggested to modulate rapid discharge events: Glacier fronts are often considered unstable on reverse bed slopes due to the increased ice discharge associated with glacial retreat into deeper-lying bedrock (Nick et al., 2009; Schoof, 2007). Records of glacier variability that precede the satellite era are needed to place the rate of changes observed during the past two decades in a longer-term context. Such information is critical to determine the frequency with which rapid discharge events possibly occur and to better identify the key factors that lead to these instabilities.

Kangerlussuaq Glacier (KG) is one of the largest outlet glaciers of the Greenland Ice Sheet, but relatively little is known concerning its history prior to satellite observations. During the Holocene, KG likely reached its maximum extent during the Little Ice Age (LIA), a cold period commonly associated with the time interval AD 1450–1850 in Greenland (Kjeldsen et al., 2015). In the inner part of KG fjord, a terrestrial lateral moraine marks the maximum ice extent of the LIA (Dyke et al., 2014; Kjeldsen et al., 2015). Since the 1930s, more detailed knowledge of KG is provided by several historical expeditions: the British Arctic Air Route Expedition between 1930–1931, The Scoresby Sound Committee's 2nd East Greenland expedition in 1932 to king Christian IX's land, The Danish Three-Year Expedition to King Christian X Land (1931–1934), and The Anglo-Danish Expedition to East Greenland (1935), which continued as the British Expedition to East Greenland (1936). Between 1932 and the 1990s, only a few front observations are available, showing a front retreat of ~5 km between 1932 and 1966 and a front advance of ~1.7 km between 1966 and 1985. Overall, between the LIA maximum and 1981 KG underwent substantial thinning of 230–260 m (Khan et al., 2014). From 1981 to 1998 the thinning of KG was minor (40–50 m), but this was followed by retreat periods of varying rates during the late 1990s and 2000s, along with thinning by more than 300 m after 2003 (Khan et al., 2014).

A drastic 5-km retreat event occurred during the winter of 2004–2005, and mass loss increased at a rate of 28 Gt/year (Bevan et al., 2012; Howat et al., 2007). Subsequently, ice discharge was at least 30% higher than before the event (Mouginot et al., 2019). Another fast retreat event (~5 km) occurred between 2016 and 2018, associated with flow acceleration and thinning near the terminus (Brough et al., 2019).

In this study, we further investigate the observations of Wager et al. (1937), who noted the loss of KG's ice tongue after expeditions in 1931 and 1935–1936. By compiling additional historical sources, including a previously unpublished aerial photo by Lauge Koch in 1933, we reveal that the ice shelf loss likely occurred as a major singular event between 1932 and 1933. We investigate whether the glacier collapse left a sedimentary imprint by analyzing fjord sediments, reconstruct changes in SSTs prior to and after the collapse, and discuss the overall implications of the collapse.

1.2. Bathymetry of Kangerlussuaq Fjord

The fjord was surveyed partially in 2010 (Dowdeswell et al., 2010) and resurveyed in 2015, this time including the inner part of the fjord (Fenty et al., 2016; NASA OMG, 2016). The fjord is on average 700–900 m deep and has a relatively smooth floor and steep side walls (Figure 1a). It is connected to Kangerlussuaq Trough, which crosscuts the shelf and reaches 650 m deep (Christoffersen et al., 2011). In the inner fjord a prominent submarine ridge is present. This ridge consists of two high-amplitude ridges that are separated by a lower amplitude, wedge-like geometry (Figure 1b; Batchelor et al., 2019). This feature is interpreted to have formed when KG was grounded at its lateral margins but floating at its central part (Batchelor et al., 2019). This submarine ridge forms a lateral extension of the terrestrial LIA moraines (Kjeldsen et al., 2015) and is thus likely a result of the LIA advance/still stand.

2. Materials and Methods

Historical evidence was gathered from the sources listed in Table 1. Four short marine sediment cores (1- to 2-m core length) were collected during a cruise in Southeast Greenland with the MV Fox in 2012 (Figure 1 and Table S1 in the supporting information). Age constraints of the sediments were achieved using the ^{210}Pb dating method. The age models were calculated based on the Constant Flux–Constant Sedimentation model (see the supporting information). X-ray images were obtained from split core halves. Cores were sampled continuously every centimeter for grain size analysis. The samples were wet sieved, separating them into three grain size fractions (<63, 63–150, and >150 μm). For the >150-μm fraction, individual grains that weighed more than 0.01 g were discarded in order to reduce distortion of the grain size signal resulting from the occurrence of singular large grains (Wangner et al., 2018). Weight percentages of the sand fraction were calculated relative to the total dry weight. Sediment weight percentages were converted to IRD fluxes

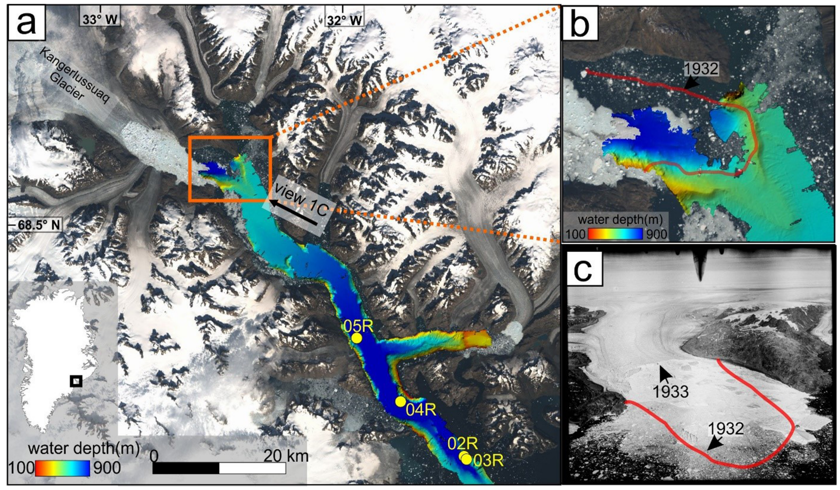

Figure 1. (a) Sentinel satellite image displaying Kangerlussuaq Fjord and its surroundings (27 August 2018). The location of the fjord in Greenland is indicated with a black box in the inset map. Sediment core locations are indicated by yellow dots, full core names include the prefix "FOX12-". The orange box indicates the position of Figure 1b. O(b) Zoom of bathymetry data displaying a large submarine moraine, marking the maximum position of the glacier during the LIA. The moraine's location corresponds to the position of the KG front in 1932. The 1932 front position is from Mikkelsen (1933). (c) Aerial photograph taken by L. Koch in 1933 showing the glacier front retreat of ~9 km relative to the year 1932 (Koch, 1933); red line indicates the position of the glacier front in 1932 (Mikkelsen, 1933; Figure S2).

(Andresen et al., 2012). Alkenone paleothermometry ($U^{K'}_{37}$ index) was applied to reconstruct the variability of surface water temperatures using the calibration of Prahl and Wakeham (1987). The BAYSPLINE calibration recently suggested by Tierney and Tingley (2018) is also presented for comparison. In the Northern North Atlantic, alkenone distributions predominantly reflect late summer temperatures (Sicre et al., 2014; Tierney & Tingley, 2018). Detailed methodology is available in the supporting information.

Table 1
List of the Historical Documents Used to Demonstrate the Collapse

Observation	Year of publication	Document type	Description of the glacier front	Expedition	Reference
1930	1937	Land-based photograph (Figure 2b)	"Floating ice tongue"	British Arctic Air Route Expedition 1930–1931	Wager, H. G. and Manley, G.: The Kangerdlugssuak Region of East Greenland, Geogr. J., 90(5), 393–421, 1937.
1931	1932	Aerial photo (Figure S1b)	No explicit description provided by the author	British Arctic Air Route Expedition 1930–1931	Watkins, H.G., 1932, The British Arctic Air Route Expedition: The Geographical Journal, v. 79, p. 353–367.
1932	1933	Topographic map (Figure S2)	"Glacier tongue"	The Scoresby Sound Committee's 2nd East Greenland expedition in 1932 to king Christian IX's land	Topographic map by M. Spender, published in: Mikkelsen, E., 1933, The Scoresbysund Committee's 2nd East Greenland Expedition to King Christian IXs land.: Meddelelser om Grønland, v. 104, p. 71.
1933	1933	Aerial photo (Figure 1c)	No explicit description provided by the author	The Danish Three-Year Expedition to King Christian X Land	Koch, L.: The Danish Three-Year Expedition to King Christian X Land, Geogr. Rev., 23(4), 599–607, 1933.
1935	1937	Land-based photograph (Figure 2c)	"Ice tongue replaced by icebergs"	Anglo-Danish Expedition to East Greenland	Wager, H. G. and Manley, G.: The Kangerdlugssuak Region of East Greenland, Geogr. J., 90(5), 393–421, 1937.

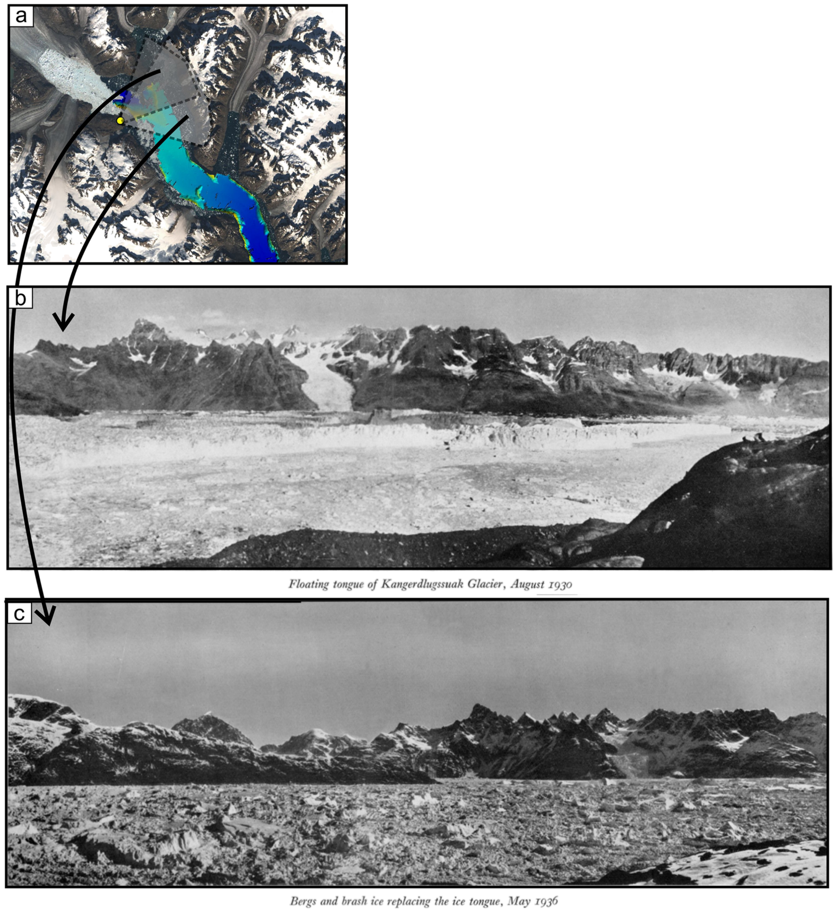

Figure 2. Overview of observations presented in Wager et al. (1937). a) Indication of the approximate position (yellow dot) from where the land-based photographs were taken, together with their approximate field of view (grey triangle). Note that the photo from 1936 was obtained with a slightly more northern orientation. b) Photograph of the floating ice tongue in August 1930. c) Photograph of the ice mélange in May 1936.

3. Results

3.1. Compilation of Historical Observations

The first direct observations of the KG's ice tongue occurred in 1930 and 1931 during the British Arctic Air Route Expedition, documented by both a land-based photograph (Wager et al., 1937; Figure 2a) and an aerial photograph (Watkins, 1932; Figure S1). Between July 1935 and August 1936, L.R. Wager revisited Kangerlussuaq fjord as part of the Anglo-Danish expedition to East Greenland. During this journey he observed that

> "*The condition of the Kangerdlugssuak Glacier was very different in 1936 from what it was in 1930. Then a floating ice tongue 5 miles long pushed out into the fjord, where it periodically gave rise to large tabular icebergs a quarter of a square mile in area (Plate 6). In 1936 the continuous floating tongue had been replaced by a jumble of smaller bergs and brash ice (Plate 7).*" (Wager et al., 1937, p. 407; Plate 6 and 7 refer to Figure 2b and 2c, respectively).

Apart from this paragraph, no further discussion or interpretations were provided and this finding has hitherto not been discussed in modern literature. By compiling additional historical sources, (Table 1) it becomes clear that the retreat observed by L.R. Wager most likely occurred as part of a massive collapse that took place between August 1932 to August 1933. In August 1932, a detailed map of the fjord depicting the position of the floating tongue was produced using terrestrial photogrammetry (Figure S2; Mikkelsen,

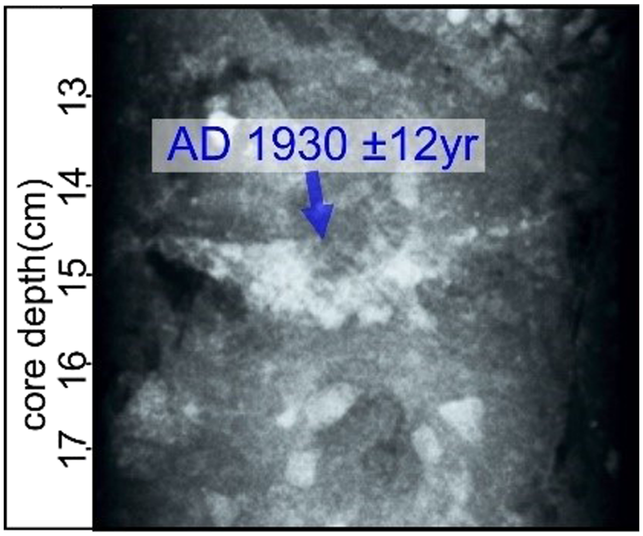

Figure 3. Close-up of X-ray image of core FOX12-02R showing an IRD layer possibly related to the glacier collapse, dated to 1930 ± 12 years (see Figure S3 for location in the core).

1933). An aerial photograph obtained in August 1933 reveals that the margin of the glacier had by then retreated by approximately 9 km and was likely grounded (Figure 1c; Koch, 1933). These observations thus pinpoint the rapid collapse of the ice tongue to have occurred between August 1932 and August 1933.

3.2.. Sedimentology and Chronology

Lead dating reveals that sediment core FOX12-02R covers the past century and thus allows comparison with the available historical observations. The chronology of cores FOX12-03R, FOX12-04R, and FOX12-05R show that these sediments are younger than 1960 (FOX12-04R, Figure S3) or contain reworked sediments (FOX12-03R and FOX12-05R, see the supporting information). Grain size analysis, X-ray imaging, and optical imaging of core FOX12-02R indicate a mud-supported diamicton with no signs of bioturbation (Figure S3). The grain size composition consists predominantly of silt and clay (60–90%) with larger clasts interspersed throughout the core. Three IRD peaks of >150 μm stand out in the record at 41, 30, and 14–16 cm (Figure S4). The IRD peaks at 41 and 30 cm do not display a peak in the 63- to 150-μm fraction but the peak at 14–16 cm is reflected in both fractions, due to a layer with a defined upper and lower boundary (Figure 3). This layer is grain supported and contains relatively little mud (54%). Measurements of excess ^{210}Pb ($^{210}Pb_{xs}$) show a decreasing trend in top 20 cm (Figure S5). Below this no $^{210}Pb_{xs}$ is present. The upper 20 cm comprises the past ~100 years, corresponding to a sedimentation rate of 0.18 cm/year (Figure S5). This sedimentation rate is somewhat lower but comparable to that observed previously in the outer part of the fjord (0.25–0.34 cm/year; Andrews et al., 1994). The top of the IRD layer at 14.5 cm is dated to 1930 ± 12 years. The lower part of the core (20–131 cm) could not be dated due to the lack of material containing ^{14}C.

3.3.. Alkenone SST Reconstruction

The reconstructed temperatures range between 6 and 11 °C, which is significantly higher than in situ SST observations (0–4 °C, 10-m water depth) measured in August 2004 (Christoffersen et al., 2011) and September 2010 (Inall et al., 2014). We attribute this offset to the advection of "warm" detrital alkenones produced in the Irminger current waters. This interpretation has been previously proposed to explain similar SST overestimations in Sermilik Fjord sediments (Andresen et al., 2013; Andresen et al., 2017). Indeed, the SST reconstruction from core FOX12-02R shows similarities with the annual mean SST record compiled from the South of Iceland serving as an indicator of Irminger Current variability (Figure S6, site A; Andresen et al., 2012). Additionally, this is also reflected in other surface water temperature records in areas influenced by the Irminger current (Figures S6 and S7). Based on this comparison, we interpret that the $U_{37}^{K'}$ temperature reconstructions predominantly reflect the variability of waters in the Irminger Current, which ultimately reach Kangerlussuaq fjord.

4. Discussion and Conclusions

4.1. Cause of the Ice Tongue Collapse

The SST reconstruction from core FOX12-02R together with climate observations from the region and bathymetric data from the fjord provides insights into the potential causes of the glacier collapse. The similarity of the SST reconstruction from core FOX12-02R with the SST compilation from South of Iceland (Andresen et al., 2012) suggests that waters within Kangerlussuaq fjord generally reflect a common regional pattern of ocean variability linked to the Irminger Current. This includes a distinct warming that occurred during the late 1920s and early 1930s, which is also present in the air temperature record from Tasiilaq (Figure 4). Temperature and salinity profiles have previously revealed the presence of Atlantic-sourced waters in the fjord (Christoffersen et al., 2011; Jackson et al., 2014). Other investigations of fjord circulation have also shown the importance of shelf water variability on the interactions between Atlantic-sourced waters and the glacier front (Cowton et al., 2016; Straneo & Cenedese, 2015). Therefore, we consider it

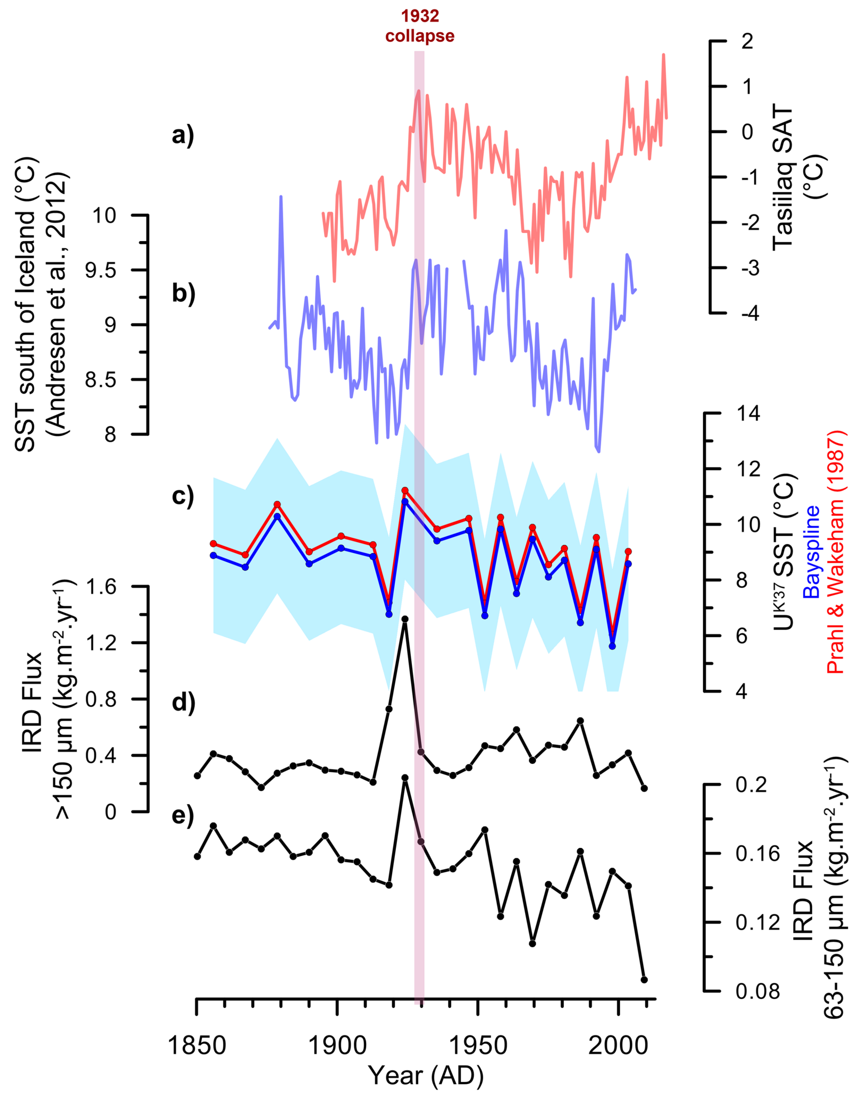

Figure 4. Comparison of core FOX12-02R data with historical climate records. (a) Annual mean air temperature from Tasiilaq (Cappelen, 2011). (b) Annual mean sea surface temperature compiled from south of Iceland, representative of the Irminger Current variability (Andresen et al., 2012). (c) Reconstructed SSTs within the Kangerlussuaq Fjord based on the calibration of Prahl and Wakeham (1987) in red and the BAYSPLINE calibration (Tierney & Tingley, 2018) in blue. Light-blue shading indicates the $\pm 2\sigma$ interval uncertainty interval related to the BAYSPLINE calibration. (d, e) fluxes of ice-rafted debris deposited on the fjord floor, measured for the size fractions >150 and 63–150 μm, respectively.

likely that warmer Atlantic Waters during the late 1920s, evident from the SST reconstruction and regional records, propagated to the glacier front, and influenced the stability of the ice tongue. The air temperature record at Tasiilaq, located 400 km southwest of KG analogously reveals relatively cold air temperatures between 1900 and 1920, followed by a rapid increase in temperatures in the 1920s. For the entirety of Greenland, the rate of air temperature warming during the 1920s was larger by a factor of 1.33 compared to 1994–2007 (Box et al., 2009). Thus, since the collapse of the ice tongue occurred during oceanic and atmospheric maxima, we infer that destabilization of the ice tongue was most likely initiated by climate warming.

To assess the role of bedrock topography and pinning points influencing the collapse, we use recently acquired bathymetry data (NASA OMG Mission, 2016). These data show a large submarine ridge (300 m above the surrounding sea floor), which consists of two moraines separated by a grounding zone wedge (Figure 1b) and is positioned right at the limit of the floating ice tongue in 1932 (Figures 1a and 1b). Due to its large size and position we suggest that the ice tongue was pinned to and stabilized by this ridge. This is consistent with the interpretation that the ridge was formed by a partially grounded, partially floating ice shelf (Batchelor et al., 2019). This would mean that unpinning from the ridge, initiated by climate warming, would have led to the sudden loss of support and buttressing, favoring a rapid collapse of the ice tongue.

4.2. Sedimentary Trace of the Collapse

The most striking change in IRD variability in core FOX12-02R is the presence of a coarse IRD layer dated to 1930 ± 12 years. This age determination indicates that deposition of the IRD layer could have been coeval with the 1932–1933 collapse. The IRD pebbles are generally embedded in a mud matrix, but in this layer the IRD is grain supported and therefore stands out as an IRD anomaly that is unique in the entire record (Figures 3 and S4). Its characteristics indicate rapid deposition of coarse IRD within a short time period. Multiple sedimentation processes could have led to the deposition of such layers. These include (i) intense IRD deposition from a high concentration of icebergs that linger in the fjord, (ii) an iceberg overturning that releases a large pulse of debris, or (iii) deposition from turbidity currents. Due to the lack of particle sorting and a fining upward sequence, turbidite deposition is excluded. Deposition related to a “random” iceberg overturning event is likely, but owing to the timing of the IRD deposition and its uniqueness in the record we suggest that a link with the glacier collapse is also probable. This could be the result of an increased concentration of icebergs within the fjord after the collapse. Although icebergs from tributary glaciers could have contributed IRD to the core site, KG has an ice velocity of one magnitude higher than all tributary glaciers combined and thus has higher potential for iceberg calving (Figure S8). Therefore, the most likely source of IRD is KG. To conclusively link the IRD layer with the glacier collapse the layer should be dated and sampled in multiple cores, but this was not possible due to turbidite deposition in the other cores in this study (see the supporting information).

4.3. Wider Implications

First, the above findings aid the understanding of the general evolution of KG during the 20th century, and second, it provides an insight into the behavior of a large ice tongue in response to climatic change. This is important as it has been questioned whether the recent collapse/decay of ice tongues in North Greenland (e.g., at Petermann Glacier; Reilly et al., 2019) are events that occur frequently or whether these represent a response to current anthropogenic warming. With regard to the 20th-century evolution of KG, its destabilization after the final phase of the LIA occurred remarkably late. For instance, Jakobshavn Isbræ in West Greenland and Kangiata Nunaata Sermia in Southwest Greenland retreated from their maximum LIA position already by 1851 (Csatho et al., 2008) and 1761 (Lea et al., 2014), respectively. While acknowledging local and regional differences, the year 1900 has been used as a Greenland-wide time stamp of the onset of glacial retreat (Kjeldsen et al., 2015). We suggest that the prolonged stability of KG could be explained by its pinning to the large submarine ridge. While many other (peripheral) glaciers in East Greenland had retreated substantially in the period 1900–1930 (Bjørk et al., 2018), the response of KG was delayed due to its pinning to the submarine moraine. When KG eventually retreated off the moraine, this resulted in a nonlinear response. Whether the collapse of KG was followed by a prompt increase in ice flow and discharge is hard to deduct, since the first front observation after 1933 stems from 1966 (Khan et al., 2014). In 1966, the front had retreated ~5 km, probably indicating a moderate retreat rate during this period, related to overall cooler conditions compared to the late 1920s/early 1930s (Figure 4).

Overall, the timing of the collapse of KG makes part of a northward trend of ice tongue break-ups at large tidewaters during the 20th century. This trend began at the start of the early 20th-century warming with the loss of the ice tongue at Helheim Glacier (66°21′N) around ~1900 (Andresen et al., 2017). Later, the KG collapse (68°38′N) occurred at the peak of the 1920s–1930s warming period. The ice tongue of Jakobshavn Isbrae (Sermeq Kujalleq, 69°10′N) retreated 11 km between 2000 and 2003 (Holland et al., 2008) in response to the ongoing warming trend that started in the 1990s. In Northern Greenland, the ice shelf of Zachariæ Isstrøm (78°20′N) disintegrated between 2007 and 2015 (Mouginot et al., 2015) and the ice tongue of Petermann Glacier (81°10′) showed large calving events in 2010 and 2012 (Reilly et al., 2019). From this overall trend, it can be deducted that the climatic window in which ice tongues can remain stable has moved northward throughout the 20th and 21st centuries. With air and ocean temperatures predicted to keep increasing, the loss of ice tongues in Northern Greenland seems inevitable in the near future, but differences in retreat timing may occur depending on their local bathymetric setting.

Overall, it is important that the nonlinear contribution to sea level rise, associated with the loss of ice tongues and potential acceleration of ice discharge at these glaciers, is accounted for in simulations of sea level rise.

4.4. Conclusions

Historical evidence is used to reveal a massive collapse of KG's ice tongue between 1932 and 1933. Observed and reconstructed temperature records show that the glacier retreat likely occurred in response to oceanic and atmospheric warming. The unpinning from a large submarine moraine also plays an important role in explaining the magnitude of the event. The deposition of a distinct IRD layer coevally with the collapse is remarkable and might represent a sedimentary trace of the collapse, although other depositional processes unrelated to the collapse cannot be excluded. Altogether, this study provides a rare insight into a past analogue of rapid destabilization of a marine outlet glacier, thereby illustrating the sensitivity of Greenlandic ice tongues to climate warming and the importance of the local physical setting to explain the differences within timing of the retreat of marine outlet glaciers.

Data Availability Statement

Sediment core data are available at https://doi.org/10.1594/PANGAEA.908232.

The bathymetric data (OMG Mission, NASA) is available at https://omg.jpl.nasa.gov/portal/browse/.

Acknowledgments
This study is a contribution to the VILLUM project "Past and Future Dynamics of the Greenland Ice Sheet: what is the ocean hiding?" (10100). A. A. B. was funded by the Carlsberg Foundation (Grant CF17-0529). We thank the CNRS for salary support of M. A. S. and V. K., and the NAIV project funded by LEFE/INSU. We thank James Lea and an anonymous reviewer for their insightful comments.

References

Andresen, C. S., Kokfelt, U., Sicre, M. A., Knudsen, M. F., Dyke, L. M., Klein, V., et al. (2017). Exceptional 20th century glaciological regime of a major SE Greenland outlet glacier. *Scientific Reports*, *7*(1), 13626. https://doi.org/10.1038/s41598-017-13246-x

Andresen, C. S., Sicre, M.-A., Straneo, F., Sutherland, D. A., Schmith, T., Hvid Ribergaard, M., et al. (2013). A 100-year long record of alkenone-derived SST changes by Southeast Greenland. *Continental Shelf Research*, *71*, 45–51. https://doi.org/10.1016/j.csr.2013.10.003

Andresen, C. S., Straneo, F., Ribergaard, M. H., Bjørk, A. A., Andersen, T. J., Kuijpers, A., et al. (2012). Rapid response of Helheim Glacier in Greenland to climate variability over the past century. *Nature Geoscience*, *5*(1), 37–41.

Andrews, J. T., Milliman, J. D., Jennings, A. E., Rynes, N., & Dwyer, J. (1994). Sediment thickness and Holocene sedimentation in 3 Greenland fjords. *The Journal of Geology*, *102*, 669–683.

Batchelor, C. L., Dowdeswell, J. A., Rignot, E., & Millan, R. (2019). Submarine moraines in Southeast Greenland fjords reveal contrasting outlet-glacier behavior since the Last Glacial Maximum. *Geophysical Research Letters*, *46*(6), 3279–3286. https://doi.org/10.1029/2019GL082556

Bevan, S. L., Luckman, A. J., & Murray, T. (2012). Glacier dynamics over the last quarter of a century at Helheim, Kangerdlugssuaq and 14 other major Greenland outlet glaciers. *The Cryosphere*, *6*(5), 923–937. https://doi.org/10.5194/tc-6-923-2012

Bjørk, A. A., Aagaard, S., Lütt, A., Khan, S. A., Box, J. E., Kjeldsen, K. K., et al. (2018). Changes in Greenland's peripheral glaciers linked to the North Atlantic Oscillation. *Nature Climate Change*, *8*(1), 48–52. https://doi.org/10.1038/s41558-017-0029-1

Box, J. E., Yang, L., Bromwich, D. H., & Bai, L.-S. (2009). Greenland ice sheet surface air temperature variability: 1840–2007. *Journal of Climate*, *22*(14), 4029–4049. https://doi.org/10.1175/2009JCLI2816.1

Brough, S., Carr, J. R., Ross, N., & Lea, J. M. (2019). Exceptional retreat of Kangerlussuaq Glacier, East Greenland, between 2016 and 2018. *Frontiers in Earth Science*, *7*(May), 1–11. https://doi.org/10.3389/feart.2019.00123

Cappelen, J. (2011). DMI monthly climate data collection 1768–2010: Denmark, The Faroe Islands and Greenland. Technical Report

Christoffersen, P., Mugford, R. I., Heywood, K. J., Joughin, I., Dowdeswell, J. A., Syvitski, J. P. M., et al. (2011). Warming of waters in an East Greenland fjord prior to glacier retreat: Mechanisms and connection to large-scale atmospheric conditions. *Cryosphere*, *5*(3), 701–714. https://doi.org/10.5194/tc-5-701-2011

Cowton, T., Sole, A., Nienow, P., Slater, D., Wilton, D., & Hanna, E. (2016). Controls on the transport of oceanic heat to Kangerdlugssuaq Glacier, East Greenland. *Journal of Glaciology*, *62*(236), 1167–1180. https://doi.org/10.1017/jog.2016.117

Csatho, B., Schenk, T., Van Der Veen, C. J., & Krabill, W. B. (2008). Intermittent thinning of Jakobshavn Isbræ, West Greenland, since the Little Ice Age. *Journal of Glaciology*, *54*(184), 131–144. https://doi.org/10.3189/002214308784409035

Dowdeswell, J. A., Evans, J., Cofaigh, Ó., & C. (2010). Submarine landforms and shallow acoustic stratigraphy of a 400 km-long fjord-shelf-slope transect, Kangerlussuaq margin, East Greenland. *Quaternary Science Reviews*. https://doi.org/10.1016/j.quascirev.2010.06.006

Dyke, L. M., Hughes, A. L. C., Murray, T., Hiemstra, J. F., Andresen, C. S., & Rodés, Á. (2014). Evidence for the asynchronous retreat of large outlet glaciers in southeast Greenland at the end of the last glaciation. *Quaternary Science Reviews*, *99*, 244–259. https://doi.org/10.1016/j.quascirev.2014.06.001

Fenty, I., Willis, J., Khazendar, A., Dinardo, S., Forsberg, R., Fukumori, I., et al. (2016). Oceans melting Greenland: Early results from NASA's Ocean-Ice Mission in Greenland. *Oceanography*, *29*(4), 72–83.

Holland, D. M., Thomas, R. H., de Young, B., Ribergaard, M. H., & Lyberth, B. (2008). Acceleration of Jakobshavn Isbræ triggered by warm subsurface ocean waters. *Nature Geoscience*, *1*(10), 659–664. https://doi.org/10.1038/ngeo316

Howat, I. M., Joughin, I., & Scambos, T. A. (2007). Rapid changes in ice discharge from Greenland outlet glaciers. *Science*, *315*(5818), 1559–1561. https://doi.org/10.1126/science.1138478

Howat, I. M., Joughin, I., Tulaczyk, S., & Gogineni, S. (2005). Rapid retreat and acceleration of Helheim Glacier, east Greenland. *Geophysical Research Letters*, *32*(22), 1–4. https://doi.org/10.1029/2005GL024737

Inall, M. E., Murray, T., Cottier, F. R., Scharrer, K., & Boyd, T. J. (2014). Oceanic heat delivery via Kangerdlugssuaq Fjord to the south-east Greenland ice sheet. *Journal of Geophysical Research: Oceans*, *119*, 631–645. https://doi.org/10.1002/2013JC009295

Jackson, R. H., Straneo, F., & Sutherland, D. A. (2014). Externally forced fluctuations in ocean temperature at Greenland glaciers in non-summer months. *Nature Geoscience*, *7*(7), 503–508. https://doi.org/10.1038/ngeo2186

Khan, S. A., Kjeldsen, K. K., Kjær, K. H., Bevan, S., Luckman, A., Aschwanden, A., et al. (2014). Glacier dynamics at Helheim and Kangerdlugssuaq glaciers, southeast Greenland, since the Little Ice Age. *The Cryosphere*, *8*(4), 1497–1507. https://doi.org/10.5194/tc-8-1497-2014

Kjær, K. H., Khan, S. A., Korsgaard, N. J., Wahr, J., Bamber, J. L., Hurkmans, R., et al. (2012). Aerial photographs reveal late-20th-century dynamic ice loss in Northwestern Greenland. *Science*, *337*(6094), 569–573. https://doi.org/10.1126/science.1220614

Kjeldsen, K. K., Korsgaard, N. J., Bjørk, A. A., Khan, S. A., Box, J. E., Funder, S., et al. (2015). Spatial and temporal distribution of mass loss from the Greenland Ice Sheet since AD 1900. *Nature*, *528*(7582), 396–400. https://doi.org/10.1038/nature16183

Koch, L. (1933). The Danish Three-Year Expedition to King Christian X Land. *Geographical Review*, *23*(4), 599–607.

Lea, J. M., Mair, D. W., Nick, F. M., Rea, B. R., Weidick, A., Kjær, K. H., et al. (2014). Terminus-driven retreat of a major southwest Greenland tidewater glacier during the early 19th century: Insights from glacier reconstructions and numerical modelling. *Journal of Glaciology*, *60*(220), 333–344.

Luckman, A., Murray, T., de Lange, R., & Hanna, E. (2006). Rapid and synchronous ice-dynamic changes in East Greenland. *Geophysical Research Letters*, *33*(3), 2–5. https://doi.org/10.1029/2005GL025428

Mikkelsen, E. (1933). The Scoresbysund Comitee's 2nd East Greenland Expedition to King Christian IXs land. *Meddelelser Om Grønland*, *104*(1), 71.

Mouginot, J., Rignot, E., Bjørk, A. A., van den Broeke, M., Millan, R., Morlighem, M., et al. (2019). Forty-six years of Greenland Ice Sheet mass balance from 1972 to 2018. *Proceedings of the National Academy of Sciences*, *116*(19), 9239–9244. https://doi.org/10.1073/pnas.1904242116

Mouginot, J., Rignot, E., Scheuchl, B., Fenty, I., Khazendar, A., Morlighem, M., … Paden, J. (2015). Fast retreat of Zachariae Isstrom, *northeast Greenland. Science*, *350*(6266), 1357–1361. https://doi.org/10.1126/science.aac7111

Nick, F., Vieli, A., Howat, I., & Joughin, I. (2009). Large-scale changes in Greenland outlet glacier dynamics triggered at the terminus. *Nature Geoscience*, *2*, 110–114. https://doi.org/10.1038/NGEO394

OMG Mission (2016). Bathymetry (sea floor depth) data from the ship-based bathymetry survey. Ver. 0.1. OMG SDS, CA, USA. Dataset accessed [2018-02-01] at https://doi.org/10.5067/OMGEV-BTYSS

Prahl, F. G., & Wakeham, S. G. (1987). Calibration of unsaturation patterns in long-chain ketone compositions for paleotemperature assessment. *Nature*, *330*(6146), 367–369.

Reilly, B. T., Stoner, J. S., Mix, A. C., Walczak, M. H., Jennings, A., Jakobsson, M., et al. (2019). Holocene break-up and reestablishment of the Petermann Ice Tongue, Northwest Greenland. *Quaternary Science Reviews*, *218*, 322–342. https://doi.org/10.1016/j.quascirev.2019.06.023

Rignot, E., Box, J. E., Burgess, E., & Hanna, E. (2008). Mass balance of the Greenland ice sheet from 1958 to 2007. *Geophysical Research Letters*, *35*(20), 1–5. https://doi.org/10.1029/2008GL035417

Rignot, E., Braaten, D., Gogineni, S. P., Krabill, W. B., & McConnell, J. R. (2004). Rapid ice discharge from southeast Greenland glaciers. *Geophysical Research Letters*, *31*(10), 2–5. https://doi.org/10.1029/2004GL019474

Rignot, E., Fenty, I., Menemenlis, D., & Xu, Y. (2012). Spreading of warm ocean waters around Greenland as a possible cause for glacier acceleration. *Annals of Glaciology*, *53*(60), 257–266. https://doi.org/10.3189/2012AoG60A136

Schoof, C. (2007). Ice sheet grounding line dynamics: Steady states, stability, and hysteresis. *Journal of Geophysical Research*, *112*, F03S28. https://doi.org/10.1029/2006JF000664

Sicre, M.-A., Weckström, K., Seidenkrantz, M.-S., Kuijpers, A., Benetti, M., Masse, G., et al. (2014). Labrador current variability over the last 2000 years. *Earth and Planetary Science Letters*, *400*, 26–32.

Straneo, F., & Cenedese, C. (2015). The dynamics of Greenland's glacial fjords and their role in climate. *Annual Review of Marine Science*, *7*(1), 89–112. https://doi.org/10.1146/annurev-marine-010213-135133

Straneo, F., & Heimbach, P. (2013). North Atlantic warming and the retreat of Greenland's outlet glaciers. *Nature*, *504*(7478), 36–43. https://doi.org/10.1038/nature12854

Tierney, J. E., & Tingley, M. P. (2018). BAYSPLINE: A new calibration for the alkenone paleothermometer. *Paleoceanography and Paleoclimatology*, *33*(3), 281–301. https://doi.org/10.1002/2017PA003201

van den Broeke, M. R., Enderlin, E. M., Howat, I. M., Kuipers Munneke, P., Noël, B. P. Y., Jan Van De Berg, W., et al. (2016). On the recent contribution of the Greenland ice sheet to sea level change. *Cryosphere*, *10*(5), 1933–1946. https://doi.org/10.5194/tc-10-1933-2016

Wager, L. R., Deer, W. A., Wager, H. G., & Manley, G. (1937). The Kangerdlugssuak region of East Greenland. *The Geographical Journal*, *90*(5), 393–421. https://doi.org/10.2307/1787969

Wangner, D. J., Jennings, A. E., Vermassen, F., Dyke, L. M., Hogan, K. A., Schmidt, S., et al. (2018). A 2000-year record of ocean influence on Jakobshavn Isbræ calving activity, based on marine sediment cores. *Holocene*, *28*(11), 1731–1744. https://doi.org/10.1177/0959683618788701

Watkins, H. G. (1932). The British Arctic Air Route Expedition. *The Geographical Journal*, *79*(5), 353–367.